Multiwavelength optical pyrometer for shock compression experiments

G. A. Lyzenga[a] and Thomas J. Ahrens

Seismological Laboratory, California Institute of Technology, Pasadena, California 91125

(Received 29 May 1979; accepted for publication 6 August 1979)

A system for measurement of the spectral radiance of materials shocked to high pressures (~100 GPa) by impact using a light gas gun is described. Thermal radiation from the sample is sampled at six wavelength bands in the visible spectrum, and each signal is separately detected by solid-state photodiodes, and recorded with a time resolution of ~10 ns. Interpretation of the records in terms of temperature of transparent sample materials is discussed. Results of a series of exploratory experiments with metals are also given. Shock temperatures in the range 4000–8000 K have been reliably measured. Spectral radiance and temperatures have been determined with uncertainties of 2%.

INTRODUCTION

Among the principal methods of modern physics for the study of the equations of state and physical properties of materials at high pressure and temperature is the technique of dynamic compression by shock waves. Several authors[1,2] have reviewed the techniques of shock compression of condensed matter, and discussed the information which may be obtained in experiments at pressures of 100 GPa or higher.

A major difficulty with the use of pressure-density-energy equation of state data obtained from shock wave experiments on various elements and compounds,[3,4] and with understanding the thermodynamics and interatomic dynamic behavior of these materials, is the general lack of knowledge of their temperatures. If the Mie–Grüneisen equation of state[1] is assumed for a material, then its shock temperature T_H is given by the simultaneous solution of the equations,

$$T_H = \int_{P_S}^{P_H} \frac{V}{C_V \gamma} dP + T_0 \exp\left[- \int_{V_0}^{V} \frac{\gamma}{V} dV \right] \quad (1)$$

and

$$P_S(V) = \frac{\gamma}{V}\left(- \int_{V_0}^{V} P_s dV + E_{tr} - P_H\left[\frac{(V_{00} - V)}{2} - \frac{V}{\gamma} \right] \right) . \quad (2)$$

P_H and P_S are the pressures along the Hugoniot and the isentrope of the material, while γ and C_V are the dimensionless Grüneisen parameter and the specific heat respectively. $E_{\rm tr}$ is the difference of specific internal energy at standard conditions for any phase transition which may occur, while V_{00} and V_0 are the standard condition specific volumes for the initial and transformed phases. An experimental measurement of T_H can therefore provide constraints on C_V and γ, both of which are essential parameters in thermal equations of state. Such measurements aid in an understanding of lattice anharmonicity,[5] melting,[6,7] and other aspects of vibrational lattice dynamics.

The present paper describes a fast (≲10 ns) time response optical pyrometer system which has been applied to the measurement of shock temperatures[8] in transparent materials to pressures of 175 GPa and over the temperature range of 4000–8000 K. The pyrometer is designed to be used in conjunction with a two-stage light-gas gun,[9] a device which is capable of accelerating projectiles to speeds of up to ~7 km/s. Strong shock waves are driven into sample materials upon impact of these high-speed projectiles in vacuums of 10^{-2} Torr.

Because typical shock experiments near 100 GPa pressure are less than 10^{-6} s in duration, the only practical means of temperature determination is a time resolved measurement of the thermal radiation emitted by the sample. Use of optics and solid-state detectors in the visible wavelength range permit temperature measurements between approximately 2000 K and 10^4 K. These limits are determined by the lower sensitivity limit of the silicon detectors, and by the increasing insensitivity of the slope of the visible Planck radiation spectrum to changes in temperature, respectively. Pioneering work in the measurement of shock temperatures by optical techniques was done by Kormer.[6,7] The present work incorporates substantial improvements in time resolution and spectral coverage over previous studies, and so allows a wider range of materials and pressures to be studied.

I. INSTRUMENT DESIGN

As described by Jones *et al.*,[9] the light-gas gun accelerates projectiles of approximately 20 g mass for impact with a target in an evacuated impact chamber, which in this case is about 1 m in diameter. The pyrometer design consists of an optical subsystem for light collection and spectral filtering, and a detection subsystem consisting of the photodetectors and associated recording electronics.

 0034-6748/79/111421-04$00.60 © 1979 American Institute of Physics

Downloaded 06 Mar 2006 to 131.215.240.9. Redistribution subject to AIP license or copyright, see http://rsi.aip.org/rsi/copyright.jsp

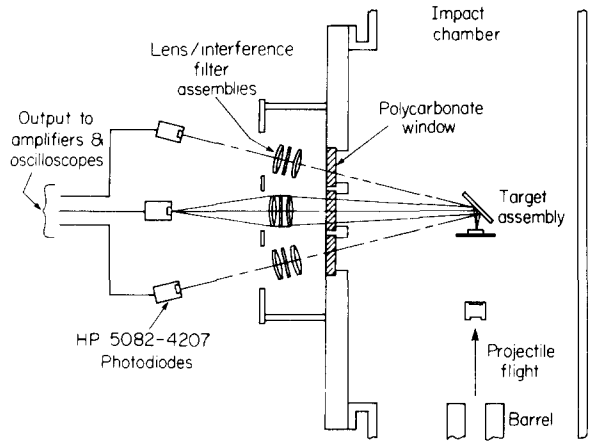

FIG. 1. Schematic drawing of pyrometer configuration.

As shown in Fig. 1, the optics are located outside the impact tank, protected by polycarbonate windows of 10 mm thickness. Six channels view the sample in a two by three rectangular array, with a window center to center distance of 9.2 cm. Each of the optical channels has a 5-cm-diam achromatic objective lens of 51-cm focal length which provides parallel light to the filter which follows in the optical path. Each filter is a narrow-band interference filter with approximately 50% peak intensity transmission and ~9-nm half-height bandwidth. The six channels span the visible and near infrared spectrum, with filters centered near wavelengths of 450, 500, 550, 600, 650, and 800 nm. Finally, an achromat of 19-cm focal length in each channel provides a filtered image of the target source at the sensitive surface of the respective photodetector.

The basic detector consists of a Hewlett–Packard 5082-4207 PIN silicon photodiode, which is reverse biased at 10 V. The diode has an active area approximately 1 mm in diameter, and produces a nominal photocurrent of 0.5 mA/mW for radiation of wavelength 770 nm. In the experimental configuration, the detector has a rated speed of response of about 1 ns. The detector is sensitive to light of wavelengths between about 400 and 1000 nm. Since the optical system produces an image of the sample which is several millimeters wide at the detector, the photodiode output current is proportional to the power per unit area radiated by the sample. It is assumed that each detector views the same region of the sample, and that the radiation flux is constant across the detected region.

As shown in the schematic diagram of Fig. 2, the photodiodes in each channel act as current sources driving 50-Ω impedance low-loss transmission lines. The signals are recorded on high-speed oscilloscopes, in this case Tektronix 585 and 7903 models. In experiments with small expected signals (less than a few mV), intermediate stages of amplification are employed. The Hewlett–Packard 8447A wide-band amplifier has been used for this purpose. The recording oscilloscopes are triggered at signal onset by the impact-generated shock wave closing self-shorting electrical contacts.[9]

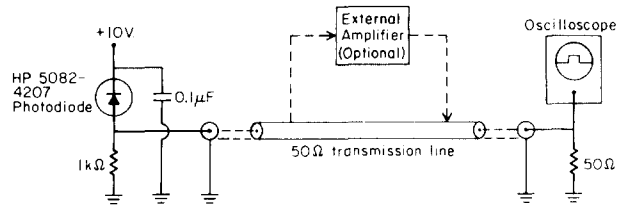

FIG. 2. Detector circuit for pyrometer channel.

Figure 3 illustrates the layout of a typical target in a shock pyrometry experiment. An expendable aluminized front-surface mirror mounted behind the sample and base plate reflects radiation to the optical channels. In the case that the investigated sample is a liquid, the target is modified to include a containment chamber and a radiation window. Alignment and focusing of the optical and detector systems prior to an experiment is achieved with the target in place. A compact light source is affixed to the target rear surface and focusing is accomplished with the interference filters removed. Positioning of the detectors within ~1 mm of the focal plane provides a detected flux reproducible to a few tenths of a percent.

Calibration of the pyrometer requires a determination of the sensitivity of each channel in its actual geometric configuration. A calibrated tungsten ribbon spectral radiance source is used in place of the target. The voltage output in this dc calibration is then used to find the voltage response for a given sample spectral radiance in power per unit area and solid angle per unit spectral bandwidth. Assuming that the detector efficiency is the same for transient and static illumination and that its intensity response is linear, the voltages measured during a shot may be interpreted directly in terms of radiation output. The calibration lamp used is a General Electric commercial type having a tungsten SR-8A filament. The lamp is calibrated by the Eppley Laboratory, Inc., Newport, RI against National Bureau of Standards calibrated standard sources. Figure 4 shows the signals expected for a blackbody source as a function of temperature, as measured for two of the actual pyrometer channels. The uncertainty in radiance calibration by the tungsten ribbon standard technique is approximately 2%.

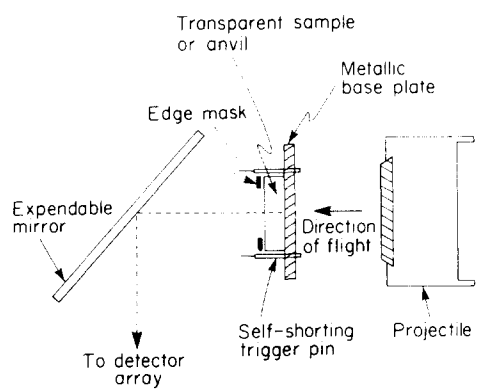

FIG. 3. Configuration of light-gas gun target.

Downloaded 06 Mar 2006 to 131.215.240.9. Redistribution subject to AIP license or copyright, see http://rsi.aip.org/rsi/copyright.jsp

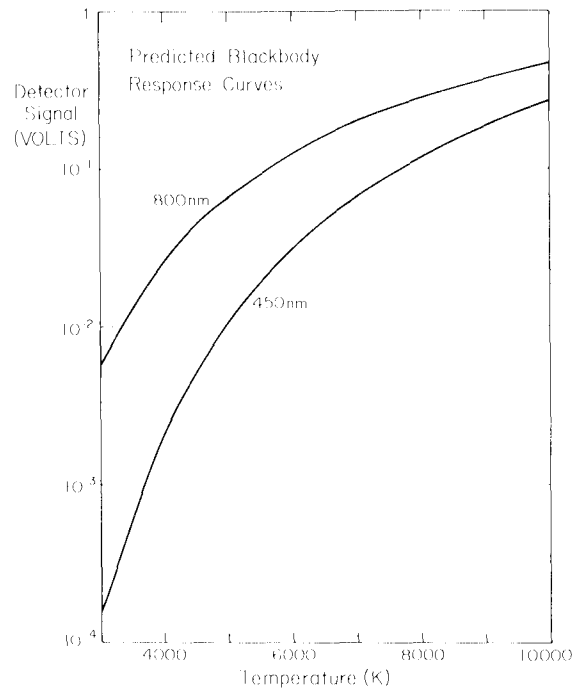

FIG. 4. Calculated pyrometer response to blackbody radiation for 800 and 450 nm channels.

II. EXPERIMENTAL RESULTS

The pyrometer has been primarily used to determine shock temperatures in initially transparent materials. This is because radiation from the heated material behind the shock front can escape through the unshocked transparent material, allowing the light to be detected during shock transit through the sample, rather than only at the instant of shock arrival at the free surface.

The materials which have been studied to date by this technique include NaCl, H_2O, SiO_2, and Mg_2SiO_4.[8] NaCl is a material whose shock temperature has been the subject of earlier work by Kormer,[6,7] and it provides a point reference from which to extend these studies. SiO_2 and Mg_2SiO_4 (quartz and forsterite) are minerals whose geophysical importance makes the characterization of their thermal equations of state significant.

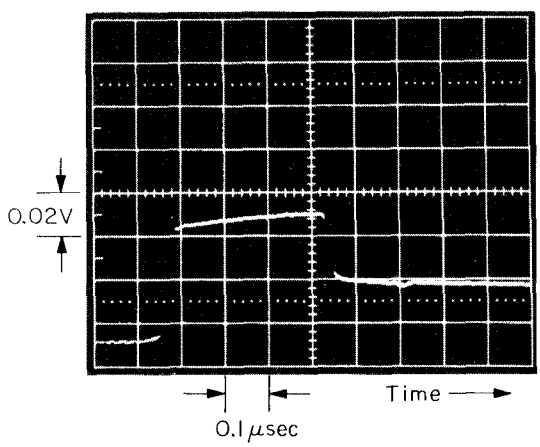

FIG. 5. Oscilloscope record for shot on fused quartz at 80 GPa pressure.

Figure 5 shows a typical experimental oscilloscope record from an experiment with quartz. The recorded light intensity rises abruptly as the shock front enters the sample, and subsequently rises more gradually, approaching an asymptotic value as the radiating layer grows in thickness. Upon arrival of the shock front at the sample free surface, the recorded intensity immediately relaxes to a value characteristic of the residual zero-pressure state of the sample. Figure 5 presents a typical experimental record, however different materials at various Hugoniot pressures have shown different detailed behavior. Some materials do not show the gradual intensity rise, but rather exhibit constant brightness throughout the shock transit. In many experiments, an initial brief flash is observed as an overshoot in the records, and is believed to be an effect of interfacial gaps between the sample and base plate.

In addition to the above described experiments, the possibility of measuring temperatures in metals has been investigated. If the metal sample is abutted with a material such as Al_2O_3, which retains its transparency under shock[10] and provides a near match in shock impedance, the metal/anvil interface temperature can be measured. A problem, however, as pointed out by Urtiew and Grover[11] arises at such an interface. The presence of a microscopic gap will introduce serious temperature disturbances and make interpretation of the data in terms of shock temperature difficult.

Figure 6 shows the results from a series of such experiments using a silver sample with Al_2O_3 anvil. In 6(a), a simple silver base plate with sapphire anvil and no interface preparation yields a decaying signal suggestive of heat diffusion from a surface temperature in-

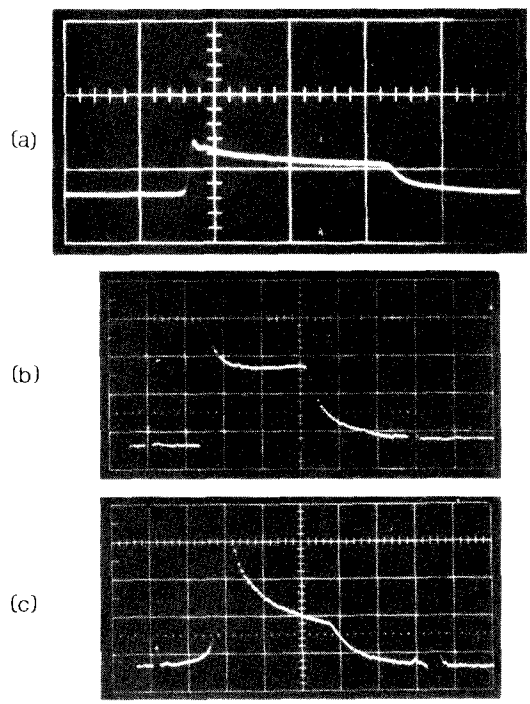

FIG. 6. Ag/sapphire composite shot records (150 GPa). (a)—sapphire anvil on polished Ag base plate; (b)—50-μm Ag coating on sapphire anvil; (c)—Ag flyer impact on bare sapphire anvil.

Downloaded 06 Mar 2006 to 131.215.240.9. Redistribution subject to AIP license or copyright, see http://rsi.aip.org/rsi/copyright.jsp

homogeneity. In 6(b), the effect has been eliminated by evaporating a silver layer onto the interface which is several tens of microns thick. This effectively eliminates the gap at the optical interface, and removes any temperature inhomogeneities to a distance over which negligible heat can diffuse during the time of the experiment. Figure 6(c) shows the unacceptable result obtained by impacting a sapphire flat directly with an Ag flyer. Surface heating effects are dominant. Thus experiments of the type 6(b) may be useful for determining shock temperatures in metals, given some additional information about the thermal diffusivities of the sample and anvil materials.

Interpretation of the pyrometer signals in terms of temperature requires comparison of the measured values of spectral radiance with a thermal radiation spectrum. At a given wavelength λ and temperature T, the spectral radiance of a blackbody is given by the Planck radiation formula,

$$N_\lambda = C_1 \lambda^{-5} (e^{c_2/\lambda T} - 1)^{-1}, \quad (3)$$

where $C_1 = 1.191 \times 10^{-16}$ W m^2/sr and $C_2 = 1.439 \times 10^{-2}$ m K. A real source which differs from the ideal blackbody case has its spectral radiance reduced by a factor $\epsilon(\lambda)$, the emissivity, which may depend upon the bulk properties of the radiating material and its surface properties.

Given the measured values of N_λ at six wavelengths in an experiment, the emissivity and temperature may be simultaneously varied to obtain the best fit of Eq. (3) to the data. In practice, an emissivity which is constant or linearly varying with wavelength is used. The emissivity is then varied to minimize the sum of the squares of deviations in temperatures calculated for each channel from the mean temperature of all channels.

Figure 7 shows the results obtained for a SiO_2 crystal experiment. The measured spectral radiance points are shown along with a Planck radiation curve fit. The curve shown is for a temperature of 4625 K and a constant emissivity of 0.68. This fit has uncertainties of approximately 2% in temperature and 7% in emissivity. Temperature determinations above ~6000 K yield less well constrained solutions because of the relative insensitivity of the visible spectrum shape to temperature in this region.

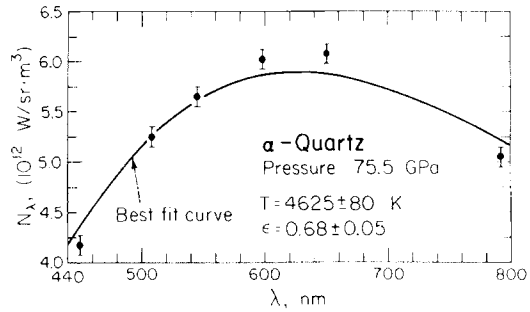

FIG. 7. Spectral radiance data and theoretical fit curve for shot on crystalline quartz.

ACKNOWLEDGMENTS

This research was supported by the National Science Foundation Grant No. EAR-7812942 and the Department of Energy. The experiments were performed at the Lawrence Livermore Laboratory light-gas gun facility. The authors are grateful for the help and encouragement of A. C. Mitchell and W. J. Nellis of the Lawrence Livermore Laboratory, and J. W. Shaner of Los Alamos Scientific Laboratory. We are grateful for the assistance of W. C. Wallace, E. Jerbic, D. Bakker, and H. Martinez. Contribution No. 3245, Division of Geological and Planetary Sciences, California Institute of Technology Pasadena, CA 91125.

[a] Supported by the Fannie and John Hertz Foundation.

[1] M. H. Rice, R. G. McQueen, and J. M. Walsh, Solid State Phys. **6**, 1 (1958).
[2] L. V. Al'tshuler, Sov. Phys. Usp. **8**, 52 (1965).
[3] J. M. Walsh, M. H. Rice, R. G. McQueen, and F. L. Yarger, Phys. Rev. **108**, 196 (1957).
[4] R. G. McQueen, S. P. Marsh, and J. N. Fritz, J. Geophys. Res. **72**, 4999 (1967).
[5] T. H. K. Barron, *Lattice Dynamics*, edited by R. F. Wallis (Pergammon, New York 1965), p. 247.
[6] S. B. Kormer, M. V. Sinitsyn, G. A. Kirillov, and V. D. Urlin, Sov. Phys. JETP **21**, 689 (1965).
[7] S. B. Kormer, Sov. Phys. Usp. **11**, 229 (1968).
[8] G. A. Lyzenga and T. J. Ahrens "Shock Temperatures of Minerals" (unpublished).
[9] A. H. Jones, W. M. Isbell, and C. J. Maiden, J. Appl. Phys. **37**, 3493 (1966).
[10] P. A. Urtiew, J. Appl. Phys. **45**, 3490 (1974).
[11] P. A. Urtiew and R. Grover, J. Appl. Phys. **45**, 140 (1974).

Downloaded 06 Mar 2006 to 131.215.240.9. Redistribution subject to AIP license or copyright, see http://rsi.aip.org/rsi/copyright.jsp